JOINT INSTITUTE FOR NUCLEAR RESEARCH

Frank Laboratory of Neutron Physics

FINAL REPORT ON THE

SUMMER STUDENT PROGRAM

Structural investigations of complex intermetallic compounds by the neutron diffraction in a wide temperature range

Supervisor:

Nadezhda Belozerova

Student:

Angelina Spiridonova, Russia
Kazan Federal University

Participation period:

June, 30 – August, 11

Dubna, 2019

Abstract

Equiatomic intermetallic alloys have been studied for a long time. For different samples the same physical properties have different degree. Their unique characteristics at the room temperature make them promising for many applications.

For this reason investigation of their crystal, electric and magnetic properties will afford to create and manage intermetallic-based devices of optic and spintronic.

The crystal and magnetic structure of complex intermetallic compounds $Mn_{0.95}Fe_{0.05}NiGe$ and MnSb has been studied by means of neutron diffraction method. All experiments by the samples studies were taken on the DN-12 diffractometer, at the IBR-2 high-flux pulsed reactor (Frank Laboratory of Neutron Physics, JINR, Dubna, Russia). Experimental data were analyzed by the Rietveld method using the FullProf software. The investigation was held at the wide range of temperatures.

As the result, the crystal and magnetic structures of $Mn_{0.95}Fe_{0.05}NiGe$ and MnSb were defined. Atomic positions, lattice parameters, interatomic bond lengths and magnetic moments were calculated for each pattern. The structural phase transition from the initial phase with hexagonal structure to the phase with orthorhombic structure at low temperature have been observed.

Introduction

Intermetallic is a large class of compounds with a wide range of physical properties. This class can be characterized by the electronic density changes near the Fermi energy and anisotropy of the crystal structure deformation. Intermetallic compounds are considered proper samples for statistic and dynamic studies as they undergo different magnetoscructural transitions and effects. Due to that, they are good matters for use in different device development. Thus, during the last years there has been noticed an increasing interest in solid-state materials which may function as magnetic refrigerators. Among physical properties of such magnetic materials may be identified the magnetocaloric effect (MCE). Based on the MCE there exist refrigeration technologies with the eliminated harmful influence[1].

One of the groups which has a significant magnetocaloric effect is the magnetic equiatomic alloys. These materials could be described with the MM'X formula where M and M' represent transition metals and X represents nonmagnetic element (Si, Ge, Sn, etc.). Over time studying of transitions in pure MM'X intermetallic it was found promising to study doped intermetallic. Nowadays, it is a huge independent field of research.

As another example there are should be mentioned intermetallic alloys, which are perspective compounds for the spintronic development[2-3]. For such goals satisfy half-metallic ferromagnetics (HMF). HMF have a giant Karr rotation of plane of polarization and could be also considered as the materials for magnetooptical recording devices[4]. An especial attention should be paid to magnetic properties of these materials.

The previous investigation on intermetallic compounds were performed, but there are many unexplored magnetic and structural characteristics. Therefore, in this work are reported the results of studying of two different promising intermetallic with the unique physical properties.

Physical properties of $Mn_{0.95}Fe_{0.05}NiGe$

Pure MnNiGe intermetallic, which belongs to the MM'X group, has been investigated as a perspective solid with a large MCE. During the studying of MnNiGe there was discovered a range of other interesting properties: magnetostructural transition, magnetoresistance, magnetic-field-induced shape memory effect and negative thermal expansion[5-6].

An especial attention was paid to the martensitic transition – a coinciding magnetic and crystallographic transition. According to [7], the doping of MnNiGe by Fe ions has changing of

temperatures of structural and magnetic transitions. Furthermore, there were observed changes related to the Fe doping level. Later it was defined that with the increasing of Fe content temperatures of transitions get lower[8].

Pure intermetallic MnNiGe has been widely explored. It belongs to the hexagonal Ni_2In-type above $T_M \approx 470$ K. At low temperature exists the structural phase transition from the initial phase with hexagonal structure to the phase with orthorhombic structure of TiNiSi-type[7-8]. At the same time, the great number of papers mention the magnetic phase transition from initial paramagnetic phase (PM) to the antiferromagnetic phase (AFM) below $T_N \approx 346$ K[7]. Doping of Mn site with the Fe atoms leads to appearing of ferromagnetism (FM).

Current investigations of this material by the neutron diffraction afford to precisely study crystal structure of $Mn_{0.95}Fe_{0.05}NiGe$. It is possible due to the ability of neutrons to separate the positions of atoms with close atomic numbers as Ni and Ge. Moreover, neutron diffraction allows observing magnetic and structural transition and establishing temperatures of respective transformations.

Physical properties of MnSb

Manganese antimonide MnSb is a half-metallic ferromagnetic compound[3]. The diversity of physical properties allow using MnSb in a different fields as development of spintronics, application as a material for electrodes. Atoms in MnSb compound arrange to the hexagonal lattice of NiAs-type space group at the RT and preserve in a wide range of temperatures[9]. Nearby to the equiatomic state ($x = 0$) $Mn_{1+x}Sb$ compound is characterized by a high homogeneity.

The substitution of MnSb or deviation from equiatomic phase cause the linear transformations of spontaneous magnetization and Curie temperature. According to [10-11], this compound has a temperature of FM-PM transition significantly above the RT (≈ 600 K).

Furthermore, the previous investigations have shown that in ferromagnetic state of MnSb, except the T_C nearby region, difference between saturation and spontaneous magnetizations are negligible. It was also found that with the temperature increasing the spin direction changes from the perpendicular to *a* to the parallel to *a* axis with the respect to *c*.

To study crystal and magnetic phases in this potential material, the neutron diffraction analysis can be used.

Methods

Neutron diffraction

The concept of the neutron diffraction is similar to the X-ray diffraction. Opened by the W.H.Bragg, W.L.Bragg and Y.V. Wulff method is based on the observation of reflected waves' maximums. As the neutrons satisfies the wave-particle duality, the diffraction of thermal neutrons on crystals may be described by the Wulff-Bragg's law.

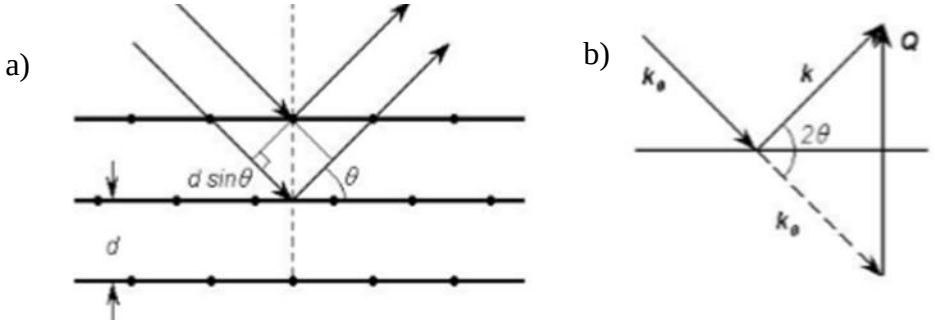

Fig. 1. Principle scheme of the Bragg reflection from the set of planes with an inter planer spacing of 'd', θ is Bragg angle (a), triangle of neutron scattering (b).

Any three dimensional periodical crystal can be divided into various sets of equidistant parallel planes, containing identical atomic arrangements. According to the Wulff-Bragg's law (1.1), constructive interference between the incident and reflected rays will be observed if the path difference between them is the integral multiple of the wavelength i.e.

$$2d \cdot \sin\theta = n\lambda \qquad (1.1)$$

where n = 0, 1, 2, 3 ... represents the order of reflection and λ – the de Broglie wavelength of neutron $\lambda = \frac{h}{mv} = \frac{h}{p} = \frac{h}{\sqrt{2mE}}$.

From the other side, presented equation (1.1) can be rewritten in another form, if the total neutron scattering is considered as an elastic one. It means that the wave vectors of incident and reflected neutrons are equal: $|\vec{k}| = |\overrightarrow{k_0}|$ (Fig. 1 (b)). Therefore, Defining the scattering wave vector $\vec{Q} = \vec{k} - \overrightarrow{k_0}$ the diffraction condition can be written as (1.2).

$$Q = |\vec{k} - \vec{k}_0| = 2k \cdot sin\theta = 4\pi \cdot sin\theta/\lambda \qquad (1.2)$$

where λ is a wavelength of incident neutrons.

Whereas that the interplanar distance and the reciprocal lattice are bound as $d = 1/|\vec{H}|$, then

$$\delta(\vec{Q} - 2\pi \cdot n\,\vec{H}) \qquad (1.3)$$

Equation (1.3) presents the other statement for the Wulff-Bragg's law.

Considering the interaction of neutrons with a nuclei by the Fermi potential $V = \frac{2\pi h^2}{m} b \cdot \delta(\vec{r} - \vec{R})$, where $\vec{R}$ is a spatial value of nuclei, it can be shown that the neutron diffraction cross section on the crystal has the following form:

$$\left(\frac{d\sigma}{d\Omega}\right)_{\text{ког}} = \frac{(2\pi)^3}{V_0} \sum_H \delta(\vec{Q} - 2\pi \cdot n) \cdot |F(\vec{H})|^2 \qquad (1.4)$$

where V_0 is a unit cell volume.

Thus, the diffraction peaks of neutron scattering, which intensity goes proportional to $\left|F(\vec{H})\right|^2$, will be observed when the scattering wave vector is a vector of the reciprocal lattice:

$$F(H) = \sum_j b_j \exp\left(2\pi \cdot i\vec{H}\vec{r_j}\right) \qquad (1.5)$$

where b_j is a coherent amplitudes of neutron scattering, $\vec{r_j}$ is coordinates of atoms in the cell.

Time of flight method

The time of flight (TOF) method is one of the main methods of the neutron diffraction analysis. Nowadays, it is one of the most efficient method in structural neutronography.

The principal scheme of a TOF diffraction experiment is shown in Figure 2.

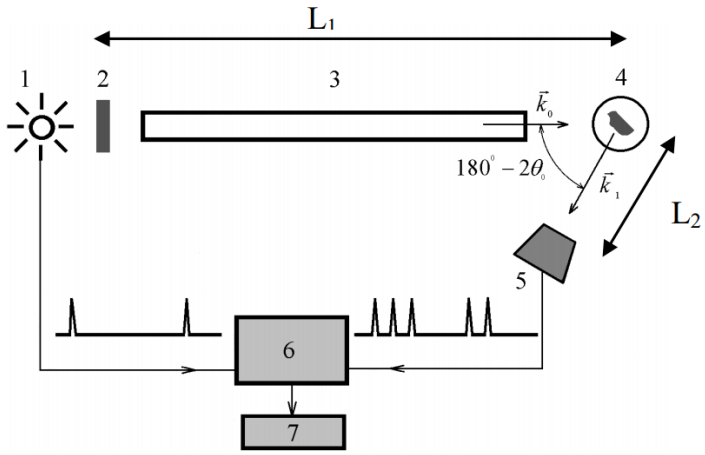

Fig. 2. The lay-out of a TOF diffraction experiment scheme: 1 – pulsed neutron source, 2 – moderator, 3 – flight path of a primary beam, 4 – sample, 5 – detector, 6 – time analyzer, 7 – RW memory.

The detector signal is stored in a multichannel time analyzer which is started synchronously with each pulse emission. The spectrum of the recorded counts is built up in dependence on neutron flight time.

From the one side, neutrons possess the kinetic moment p

$$p = mv = \frac{h}{\lambda} \tag{1.6}$$

where m is the neutron mass and v is its velocity. In this way the wavelength of neutron

$$\lambda = \frac{h}{mv} \tag{1.7}$$

On the other hand, the velocity of neutrons can be obtained from measurement of their flight times t:

$$v = \frac{L_1 - L_2}{t} \tag{1.8}$$

Thus, the wavelength of neutron can be written as

$$\lambda = \frac{ht}{m(L_1 + L_2)} \tag{1.9}$$

The reflection occurs from set of parallel crystalline planes with Miller indices (*hkl*) at a fixed θ_0 and λ. The interplanar distance d_{hkl} should measure up the Wulff-Bragg's low:

$$2d_{hkl}sin\theta_0 = \lambda \tag{1.10}$$

Thus, from (1.9) and (1.10) have

$$d_{hkl} = \frac{ht}{2m(L_1 + L_2)sin\theta_0} \tag{1.11}$$

Scattered neutrons corresponding to defined d_{hkl} can be easily separate due to the registration time. The time of each neutron flight is fixing by the time analyzer, characterized by the number of time channels and their width. The reference-start point corresponds with the special start pulse coincided with a neutron flare. Neutron diffraction patterns, obtained in such way, represent time-resolved diffraction spectra. The range of wavelengths widely used on the TOF diffractometers is generally 0,9 – 8Å. In real life it can achieve 20 Å and compensate the reduction of neutron flux at long wavelengths.

The resolution of TOF diffractometer is given as

$$R = \frac{\Delta d}{d} = (\left(\frac{\Delta t}{t}\right)^2 + (ctg\theta\Delta\theta)^2)^{1/2} \tag{1.12}$$

where Δt is equivocation of time of flight and $\Delta\theta$ is geometric equivocation of dispersal process.

Experimental results and discussion

Neutron powder diffraction measurements for complex intermetallic compounds $Mn_{0.95}Fe_{0.05}NiGe$ and MnSb were performed on the DN-12 diffractometer at the IBR-2 high-flux pulsed reactor (FLNP JINR, Dubna, Russia). Diffraction patterns were collected at scattering angle 90° with the resolution $\Delta d/d=0.022$ at d = 2 Å. Experimental data were analyzed by the Rietveld method using the FullProf software[12].

Fig. 3. Photography of DN-12 diffractometer.

Crystal structure of $Mn_{0.95}Fe_{0.05}NiGe$

Doped intermetallic compound $Mn_{0.95}Fe_{0.05}NiGe$ at the RT has hexagonal structure of $P6_3/mmc$ (№ 194) space group (Ni_2In-type). Analysis of the neutron diffraction spectra afforded to calculate lattice parameters a = 4.08 Å and c = 5.38 Å. The atomic positions were found as 2*a* (0, 0, 0) for the Mn and Fe atoms and 2*d* $(\frac{1}{3}, \frac{2}{3}, \frac{3}{4})$ and 2*c* $(\frac{1}{3}, \frac{2}{3}, \frac{1}{4})$ for the Ni and Ge, respectively. All these values are in a good agreement with the literature data[1, 12-13].

The pattern was investigated at 7 temperature points: 300 K, 270 K, 265 K, 250 K, 200 K, 100 K and 20 K. Due to the neutron diffraction there was registered a transition from initial phase with hexagonal structure to the phase with orthorhombic structure of *Pnma* (№ 62) space group

(TiNiSi-type). The schematic unit cells structure and certain diffraction spectra are presented at the Fig. 4 and Fig. 5, respectively.

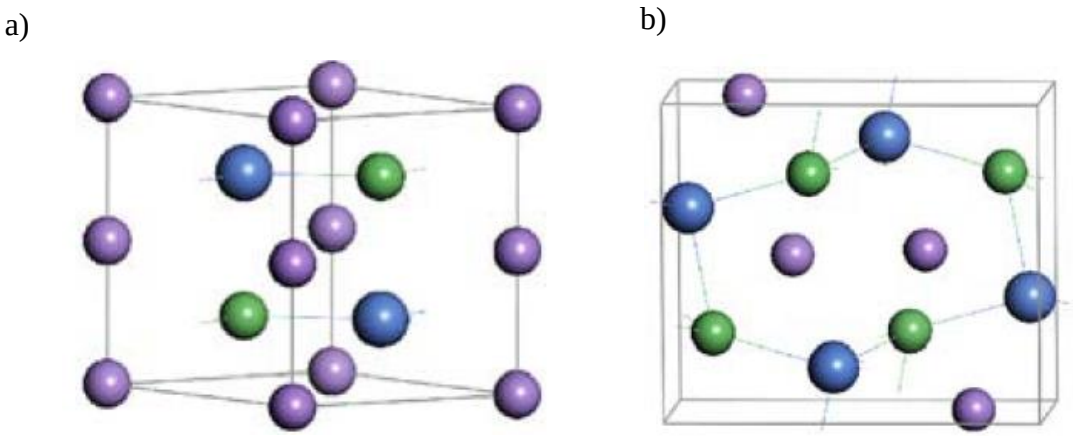

Fig. 4. Unit cells of $Mn_{0.95}Fe_{0.05}NiGe$ in a) hexagonal Ni_2In-type phase and b) orthorhombic TiNiSi-type phase, where purple atoms are Mn and Fe, blue are Ni and green are Ge.

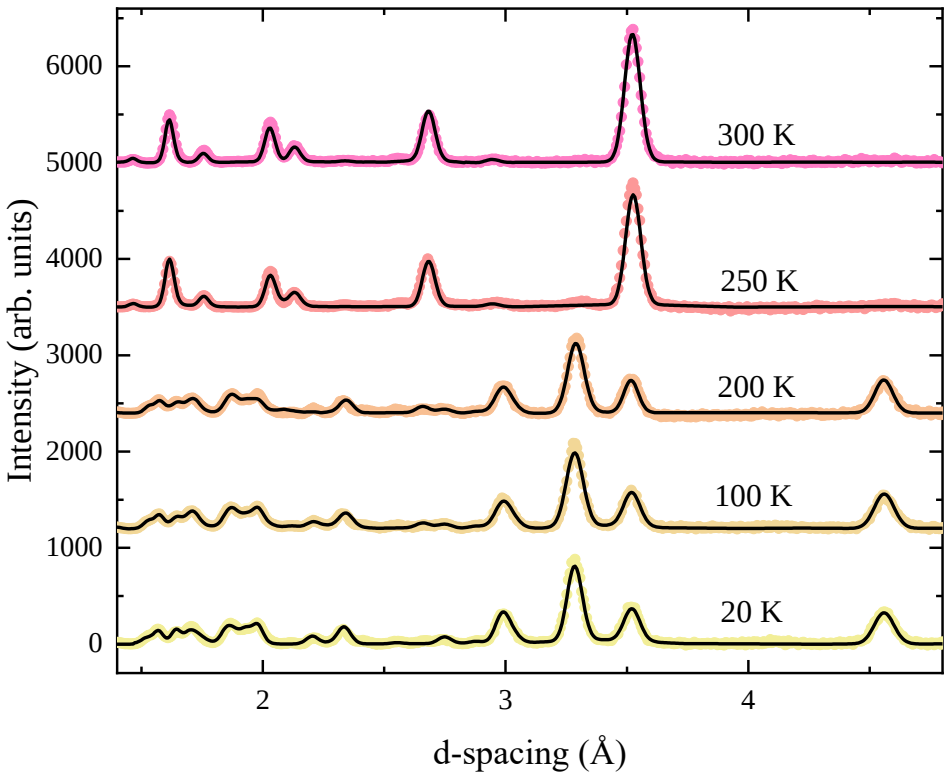

Fig. 5. The neutron diffraction spectra of $Mn_{0.95}Fe_{0.05}NiGe$ obtained at selected temperatures.

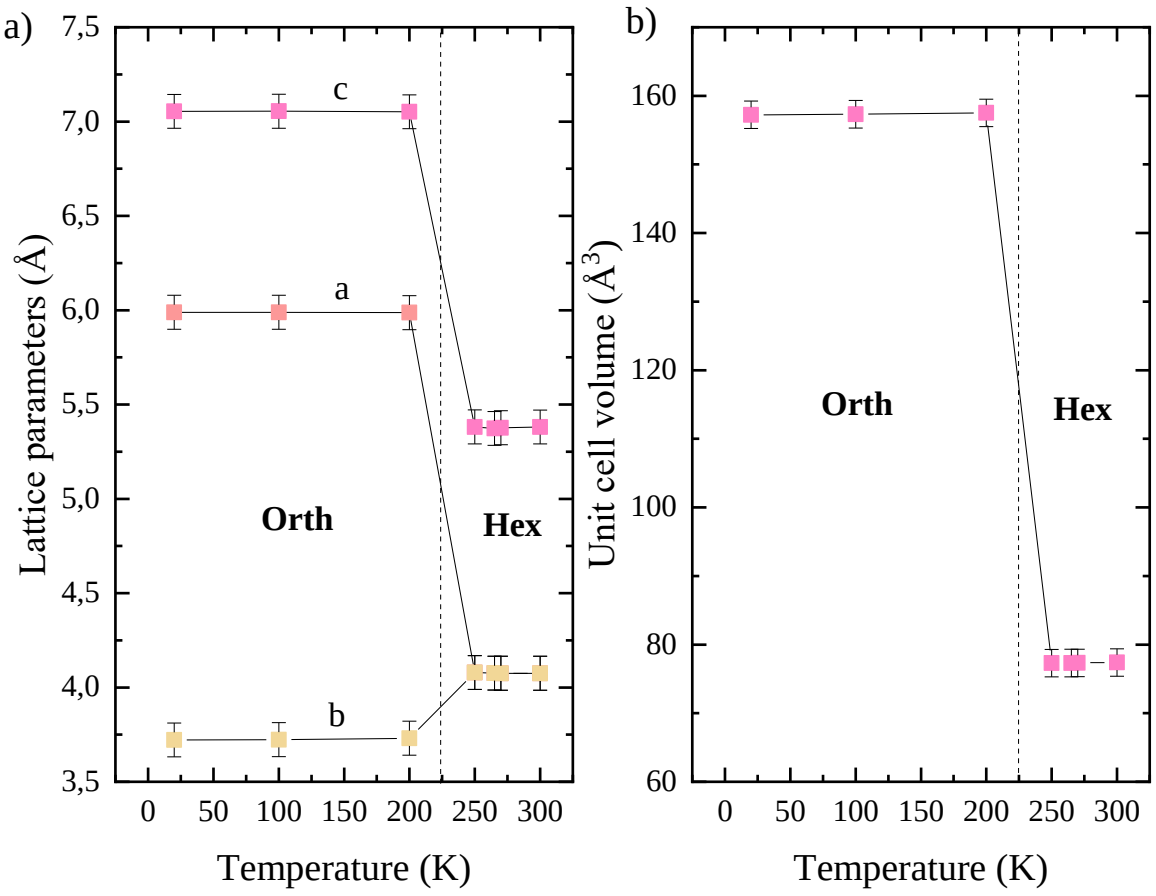

Fig. 6. Temperature dependences of lattice parameters (a) and the unit cell volume (b).

The obtained dependences of lattice parameters are in a good agreement with the previous $Mn_{0.95}Fe_{0.05}NiGe$ investigation[1]. The volume of the unit cell in the orthorhombic phase exceeds the volume in the hexagonal phase approximately in two times.

According to literature, the $Mn_{0.95}Fe_{0.05}NiGe$ sample must undergo the PM to FM/AFM transition with the temperature decreasing. As it was noted, pure MnNiGe pattern has only PM-AFM transition but for the Fe-doped patterns it is not surprisingly to observe the FM phase[7-8, 13]. However, for the current $Mn_{0.95}Fe_{0.05}NiGe$ sample any magnetic transition was not registered. Thus, it is fair to suppose that considered pattern was in the single paramagnetic state.

Crystal structure of MnSb

Intermetallic compound MnSb has single hexagonal structure of *P*6$_3$/*mmc* (№ 194) space group. Considered pattern belongs to the NiAs-type compounds and do not undergo crystallographic transition due to the neutron diffraction data analysis. This result is in a good agreement with the previous investigations of MnSb[9,14]. Experimental spectra are shown on the Fig. 7.

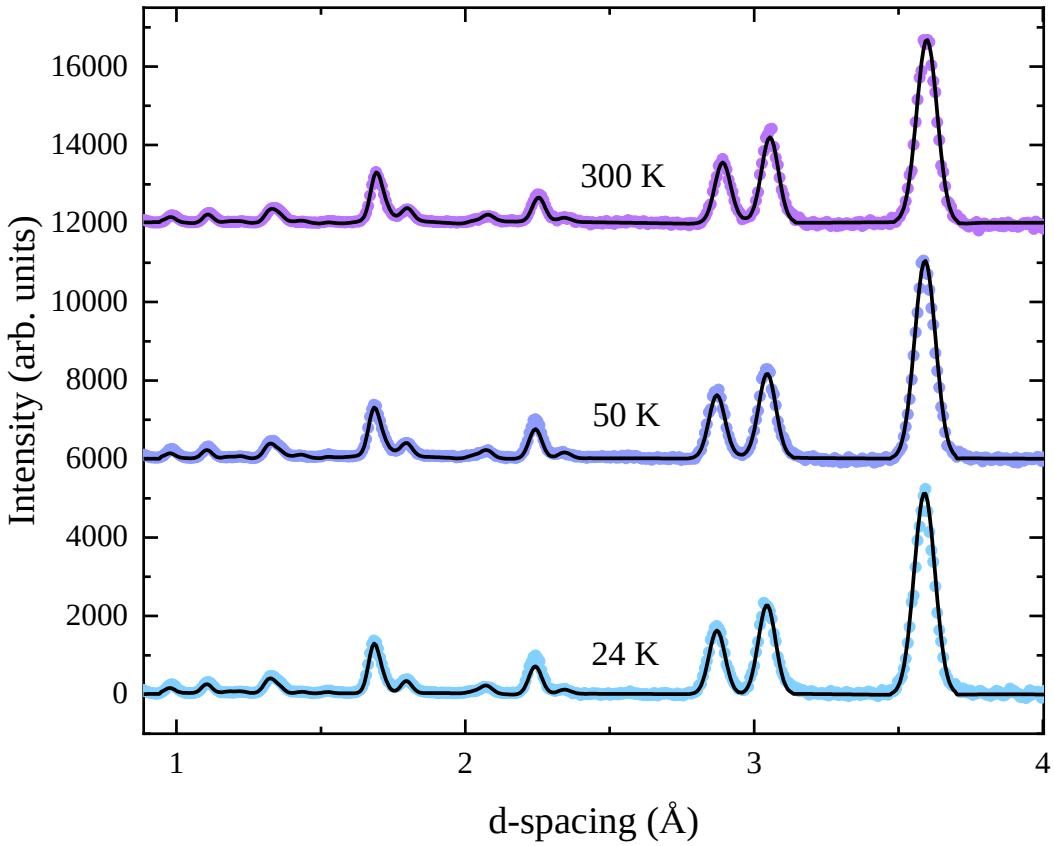

Fig. 7. The neutron diffraction spectra of MnSb pattern, obtained at the different temperatures.

Atomic positions were found as *2a* (0, 0, 0) for Mn and ($\frac{2}{3}$, $\frac{1}{3}$, $\frac{1}{4}$) for Sb. Using the FullProf software and the Rietveld method for the refinement, the lattice parameters were found as a = 4.16 Å and c = 5.79 Å. Temperature dependences of the lattice parameters and the unit cell volume are presented on the Fig. 8(a) and 8(b), respectively.

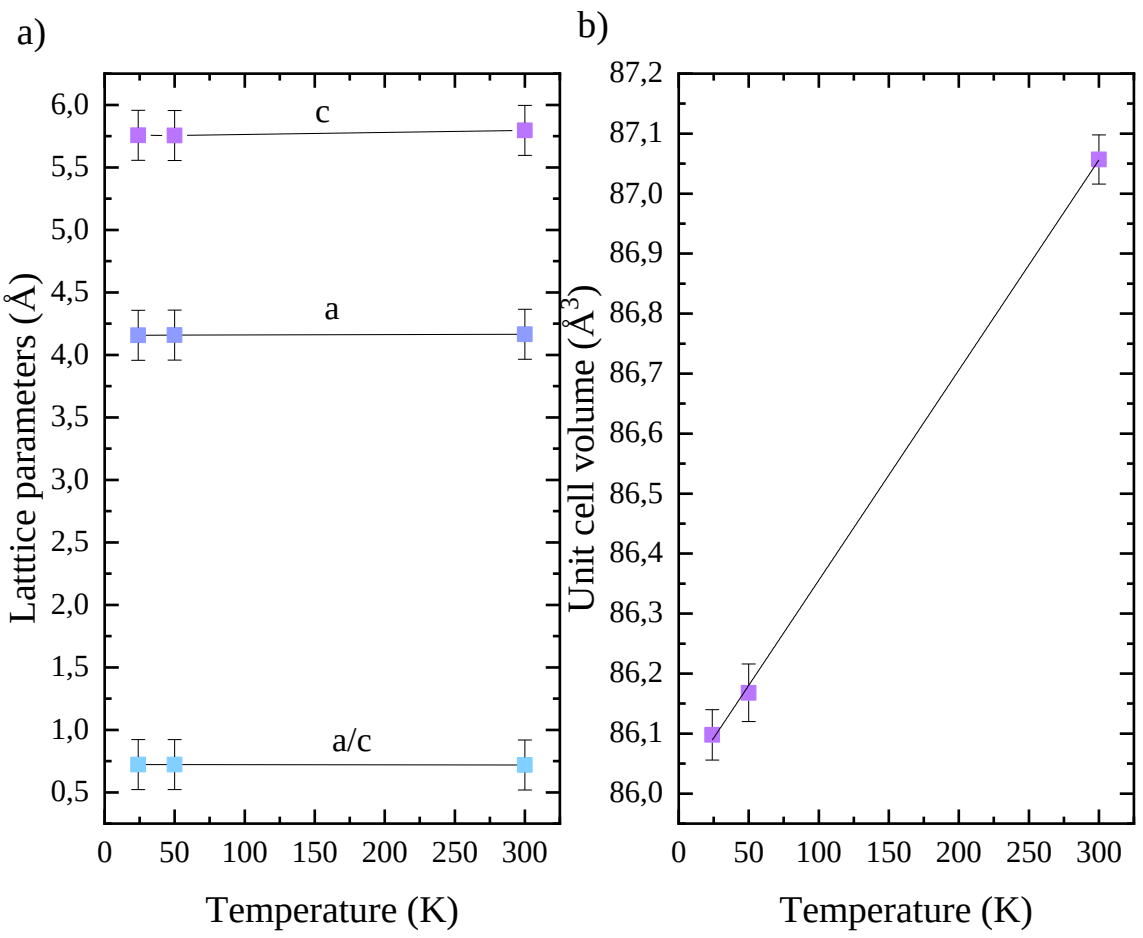

Fig. 8. Temperature dependences of lattice parameters (a) and the unit cell volume (b).

Due to the obtained data of crystal parameters, there were defined the interatomic distances. The results are presented in the Table 1. On the Fig. 9 these boundaries are shown with the black solid lines.

Table 1. The interatomic distances (Å) of MnSb compound.

Atoms\Temperature	300 K	50 K	24 K
Mn-Mn	2.8976	2.8776	2.8779
Mn-Sb	2.8074	2.7988	2.7980

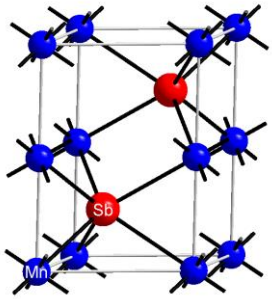

Fig. 9. Crystal structure of the MnSb sample.

Magnetic structure of MnSb

The magnetic structure of MnSb at the room temperature is presented by ferromagnetic type ordering. On the Fig. 10 is presented temperature dependence of magnetic moments. The calculated magnetic moment of Mn ions at 24 K stands at 3.28 μ_B, that is in a good agreement with the previous studies. The average value of magnetic moment for the MnSb compound is in 3 to 5 μ_B by the literature data[3,10]. Spins of magnetic Mn atoms are oriented perpendicular to the *c* axis.

The magnetic phase transition FM-PM was not observed. The ferromagnetic ordering preserves in the whole range of temperatures. According to [10-11], the T_C estimates around 600 K.

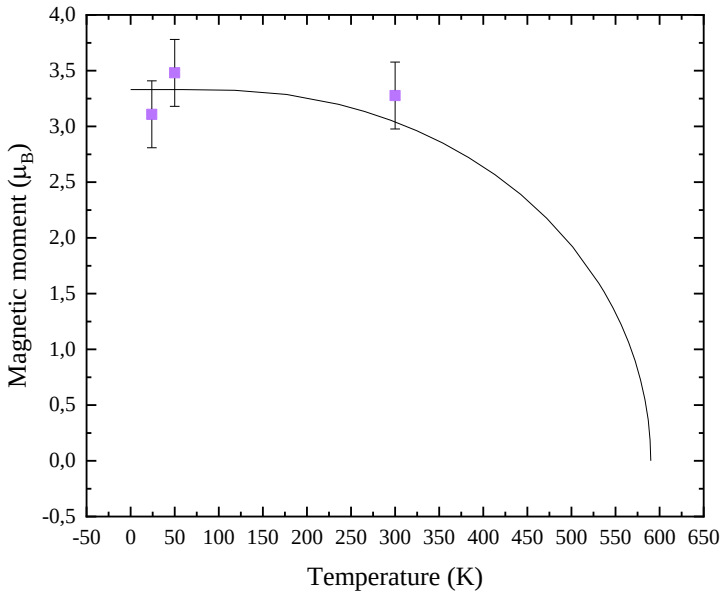

Fig. 10. Magnetic moment temperature dependence.

Conclusion

In this work were studied intermetallic alloys $Mn_{0.95}Fe_{0.05}NiGe$ and MnSb. Neutron powder diffraction measurements for each of them were performed on the DN-12 diffractometer at the IBR-2 high-flux pulsed reactor (FLNP JINR, Dubna, Russia). Experimental data were analyzed by the Rietveld method. In the course of this work, the technique of processing experimental data and FullProof software were mastered. The main characteristics of crystal and magnetic structure were calculated for different temperatures. The lattice parameters, cell volume, bond distances in three different positions were determined by the diffraction spectra analysis.

As for both of the samples the magnetic transition was not registered at the existing range of temperatures, it is perspective to investigate these patterns at different pressure. Presence of full information will afford to summarize data and define concrete temperatures of transitions.

Acknowledgement

I take this opportunity to express my profound gratitude and kind regards to my supervisor N. M. Belozerova for her exemplary guidance, monitoring and constant encouragement throughout the course of this project.

I also take the opportunity to express my deep sense of gratitude to A. V. Rutkauskas, E. V. Lukin, S. E. Kichanov and the whole team of DN-12 group for their valuable discussions, guidance and advice which helped me complete this task through various stages.

Lastly, I would like to thank a committee of Summer Student Program for opportunity to visit Joint Institute for Nuclear Research and for financial support.

References

1. M. Kristiansen, Master's Thesis (2017).
2. S. J. Jenkins, Physical Review B 70, 245401 (2004).
3. J. C. Zheng, J. W. Davenport, Physical Review B 69, 144415 (2004).
4. V. Yu. Irkhin, M. I. Katsnelson, Physics-Uspekhi 164, 705-724 (1994).
5. W. Zhao, Y. Sun, K. Shi et al., Frontiers in Chemistry 6, 15 (2018).
6. P. Dutta, S. Pramanick, D. Venkateshwarlu et al., Frontiers in Physics 108, 17012 (2014).
7. P. Dutta, S. Pramanick, S. Majumdar et al., Journal of Magnetism and Magnetic Materials 395, 312-315 (2015).
8. E. Liu, W. Wang, L. Feng et al, Nature Communications 3, 873 (2012).
9. B. T. M. Willis, H. P. Rooksby, Proceedings of Physical Society B 67, 290-296 (1954).
10. T. Okita, Y. Makino, Journal of the Physical Society of Japan 25, 1 (1998).
11. V. I. Mitsiuk, V. M. Ryzhkovskii, T. M. Tkachenka, Journal of Alloys and Compounds 467, 268-270 (2009).
12. P. Dutta, S. Pramanick, V. Singh et al., Physical Review B 93, 134408 (2016).
13. S. C. Ma, Y. Su, M. Yang et al., Journal of Alloys and Compounds 629, 322-325 (2015).
14. W. J. Takei, D. E. Cox, G. Shirane, Physical Review 129, 5 (1963).